remote sensing

MDPI

Article

When Geophysics Meets Geomatics and Archeology: Revealing the Connection Between Surface and Buried Structures at Iuvanum Archeological Site

Donato Palumbo [1], Samuel Bignardi [1,2], Oliva Menozzi [3], Patrizia Staffilani [3] and Massimiliano Pepe [1,2,*]

[1] Department of Engineering and Geology (InGeo), "G. D'annunzio" University of Chieti-Pescara, 65127 Pescara, Italy; donato.palumbo@alumni.unich.it (D.P.); samuel.bignardi@unich.it (S.B.)
[2] UDA-TECHLAB Research Center, 66110 Chieti, Italy
[3] Department of Humanities, Arts and Social Sciences, "G. D'annunzio" University of Chieti-Pescara, 65127 Pescara, Italy; oliva.menozzi@unich.it (O.M.); patrizia.staffilani@unich.it (P.S.)
* Correspondence: massimiliano.pepe@unich.it

Highlights

A multidisciplinary workflow is presented to investigate the Iuvanum archeological area by merging near-surface observations and subsurface geophysical data within a single, georeferenced 3D environment. UAV photogrammetry products (DSM/orthomosaic) provide an accurate spatial framework for positioning GPR profiles acquired on uneven terrain and for topography-corrected 3D visualization. Volumes of interest (VOIs) extracted from the assembled GPR dataset are compared with a virtual architectural model to refine interpretation and support archeological decision-making.

What are the main findings?

- Geophysical GPR results are integrated with geomatics (UAV photogrammetry/DEM/orthophoto) and archeological–architectural analysis to connect visible remains with buried structures at the Iuvanum site.
- A georeferenced 3D workflow assembles topography-corrected, non-grid GPR profiles and extracts volumes of interest (VOIs) that delineate buried walls, pavement levels, and complex features (e.g., a stair).

What are the implications of the main findings?

- The shared 3D visualization environment improves interpretability and confidence in non-invasive prospection, providing clear, prioritized targets to support excavation planning.
- The proposed workflow is reproducible on complex terrain and is readily extensible to additional geophysical datasets within the same integrated 3D framework.

Check for updates

Academic Editor: David Gomez-Ortiz

Received: 23 February 2026
Revised: 12 March 2026
Accepted: 16 March 2026
Published: 18 March 2026

Copyright: © 2026 by the authors. Licensee MDPI, Basel, Switzerland. This article is an open access article distributed under the terms and conditions of the Creative Commons Attribution (CC BY) license.

Abstract

This study presents a multidisciplinary investigation of the archeological site of Iuvanum (Abruzzo, central Italy), integrating geophysics, geomatics, architectural analysis and archeology with the purpose of exploring the relationship between surface remains and buried structures of archeological value. This research focuses on the area covering part of the forum and part of the basilica, where ground-penetrating radar (GPR) surveys were conducted to detect subsurface anomalies potentially associated with unexcavated architectural features. GPR line scans were acquired under complex topographic conditions, processed, and assembled into a three-dimensional representation, from which volumes of interest (VOIs) were extracted. These geophysical results were integrated into a comprehensive

three-dimensional framework together with high-resolution UAV photogrammetry, digital elevation models, orthophotos and a virtual architectural model (VAM) of the site. The integrated visualization environment greatly facilitates the recognition of spatial relations between the detected anomalies and the hypothesized architectural elements. The observed GPR anomalies confirmed wall remains that were initially speculated or located along their geometrical continuation. Pavement levels, as well as some structures asymmetrical with respect to the purely geometric reconstruction, were also identified. This study demonstrates how integrating GPR with geomatic and archeological approaches improves the reliability and interpretative depth of non-invasive archeological prospecting. The proposed workflow provides a reproducible methodological framework propedeutical to excavation planning and suitable for the integration of information from multi-data sensors.

Keywords: ground-penetrating radar; archeological prospection; geomatics; 3D reconstruction; Iuvanum

1. Introduction

Ground-penetrating radar (GPR) is probably the most popular geophysical technique in archeology, as it enables the detection of buried features and stratigraphic variations without excavation [1]. By transmitting short electromagnetic pulses into the subsurface and recording the back-reflected signals, GPR provides high-resolution images, where the reflected amplitude depends on contrasts in dielectric permittivity at transitions between different materials. As such, GPR is ideal for detecting the regular boundaries associated with anthropogenic structures such as walls, floors, or tombs [2,3]. Its capability to reveal spatially continuous features over large areas makes it invaluable for locating previously unknown structures and for guiding targeted excavations [4,5]. Resolution and depth of investigation of a GPR survey depend on both environmental and methodological factors among which antenna frequency, soil type, and moisture content are key players [6]. Optimal conditions, typically dry, low-conductivity sediments and strong dielectric contrasts, enable greater signal penetration and clearer imaging of archeological anomalies [7]. Conversely, clay-rich or water-saturated soils often reduce penetration and distort reflections, complicating interpretation. Modern GPR systems, however, increasingly mitigate these limitations through multi-frequency antennas, dense survey grids, and advanced signal-processing workflows [8–11].

The interpretative potential of GPR surveys is greatly enhanced when radar data are integrated with complementary geomatic and geophysical techniques, including high-precision topographic surveys, and magnetic or electrical resistivity prospecting [12,13]. Integrating these diverse datasets within a GIS framework allows radar reflections to be precisely aligned with excavation results, aerial imagery, and historical maps, producing a coherent and multi-layered representation of the site. This combined approach not only increases the accuracy of feature detection but also provides a richer contextual understanding of the archeological remains, revealing spatial patterns and relationships that would be difficult to discern using any single method alone [7,8]. In practice, such multidisciplinary synergy has enabled the detailed mapping of complex architectural layouts, buried structures, and stratigraphic sequences, demonstrating that integrating GPR with other techniques substantially enhances both the reliability and interpretative depth of archeological prospection.

Despite its strengths, it must be emphasized that radar reflections can only highlight dielectric permittivity contrasts rather than direct material identifications. As such, radar images require expert interpretation. Additionally, back-scattered waves are detected effi-

ciently when specular reflections are generated, so that the patterns observed in a radar scan do not necessarily reflect the actual geometry of the targets or the entire object being illuminated. As such, great care is needed during the interpretation when partially illuminated complex shapes are involved. In addition, phenomena such as multipath reflections, diffusion, and cluttering further complicate the interpretation task [2]. For this reason, validation through selective excavation or coring remains fundamental to confirm the archeological nature of detected anomalies [14]. Nevertheless, when integrated within a rigorous methodological framework, GPR stands as one of the most effective tools for discovering and documenting previously unknown subsurface structures [10,11]. Recent geophysical investigations, indeed, have demonstrated the effectiveness of GPR in detecting shallow archeological features and buried structures. In Babylon, for example, one of the most significant centers of ancient Mesopotamian civilization, GPR surveys have been applied to identify subsurface remains associated with domestic architecture near the Ishtar Temple; the study by Al-Assadi and Abd [15] highlights how high-resolution radargrams, maps, and 3D visualizations can reveal wall alignments and artifact distributions, providing crucial data to guide subsequent excavations. Similar research in the Borsippa site, Babylon, conducted by Kareem and Abd [16], confirmed the capability of a 250 MHz GPR system to detect wall foundations and buried architectural elements at depths of 1–3 m, contributing valuable information for local heritage management. Piroddi and Rassu [17] employed GPR to investigate hidden architectural stratifications within the San Leonardo de Siete Fuentes church in Sardinia (Italy), demonstrating the technique's potential for studying construction phases in standing monuments. Likewise, Paoletti et al. [18] applied GPR at the Etruscan necropolis of Sasso Pinzuto in Tuscania (Central Italy), successfully mapping tomb chambers and burial layouts beneath the surface. These are but a few of the many successful applications that have led the archeological community to appreciate this geophysical technique as a powerful and versatile preliminary tool for archeological prospection, enabling the non-invasive documentation of buried cultural heritage prior to large-scale excavation.

The present paper aims to follow and expand this research direction by applying GPR in combination with geomatic surveying, architectural analysis, and archeological methods. Differently from previous studies, we built a 3D environment to visualize and cross-compare geophysical, archeological, and geomatic products. Radar scans, in particular, were collected over rough terrain and along a set of non-parallel lines, which required special handling. The workflow that led to this comprehensive 3D visualization strategy can be expanded, potentially, to other kinds of datasets. Our experience emphasizes how a multidisciplinary perspective allows not only the detection of previously unknown subsurface structures, but also their precise spatial documentation, interpretation within architectural and archeological contexts, and support for informed excavation strategies.

2. Materials and Methods

2.1. A Multidisciplinary Framework for Archeological Investigation

The methodological framework adopted in this study is based on a multidisciplinary approach that integrates geophysical, geomatic, architectural, and archeological perspectives. Each professional contributes specific skills and interpretive perspectives that, when combined, allow for a more accurate, contextual, and meaningful reconstruction of the site. This synergy allows for a comprehensive understanding of the site, combining the subsurface information obtained through GPR with precise spatial data from geomatic surveys, detailed architectural analyses, and contextual archeological interpretation.

Figure 1 summarizes the interdisciplinary workflow adopted in this study, where geophysicists, geomatics specialists, and archeologists work in a continuous feedback loop

to converge on a shared interpretation. Rather than a linear sequence of tasks, the process is iterative and dialog-driven: geophysical prospection provides subsurface anomalies and preliminary targets; geomatics supplies a precise spatial framework for acquisition, referencing, and data integration; and archeological expertise contextualizes and evaluates the plausibility of the detected patterns. The mutual comparison of results across disciplines, represented by the circular arrows, supports progressive refinement of hypotheses and reduces interpretative ambiguity, ultimately enabling a more robust identification of architectural structures.

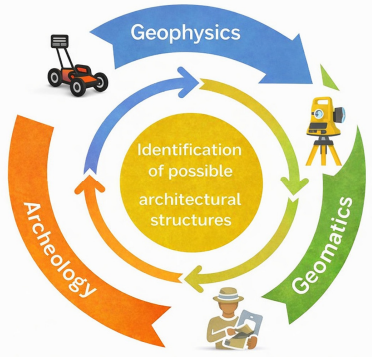


Figure 1. Conceptual diagram of the iterative, multidisciplinary approach used for identifying potential architectural structures.

The several professional figures are interconnected in a recursive manner: preliminary geophysical results guide targeted geomatic acquisitions. Furthermore, geomatics is not intended as a simple static metric support, but as an active component in the iterative process between geophysics and archeology. The spatial accuracy ensured by geomatics enhances the reliability of architectural interpretation, architectural hypotheses are evaluated against archeological knowledge, and archeological considerations, in turn, refine subsequent geophysical investigations. The circular interaction among disciplines, represented by the feedback arrows in Figure 1, ensures continuous cross-validation of data and interpretations. In this paper, first we discuss the creation of a preliminary 3D model of the entire village of Iuvanum. The creation of this model, performed with continuous interaction with our archeological group, relied heavily on geomatic techniques and besides geomatic data, it incorporated all the historical information available and results from a previous large-scale magnetic survey. Subsequently, we focus our attention on a portion of two structures, the basilica building and the forum. At this stage, this portion of the VAM accounted only for excavation evidence, available for a symmetrical part of the structures, together with the assumption of symmetry—the latter motivated by historical considerations and visible surface remains. However, the basilica/forum area had never been investigated using ground-penetrating radar or other high-resolution geophysical methods. This motivated the present GPR survey. To avoid interpretative bias, the geophysicist conducting the GPR analysis was not informed of the preliminary architectural model during the interpretation phase, nor of any other archeological information. At a later stage, geomatic, geophysical, and archeological information were integrated and jointly interpreted. This integrated interpretation is now guiding future excavation activities, which are currently being planned, and will ultimately lead to further improvements of the overall 3D model. This iterative collaboration across different fields of expertise reduces interpretative ambiguity, progressively refines the research questions, and improves the reliability of archeological reconstructions under investigation

2.2. Archeological Investigation

A key component of any archeological study is a systematic review of existing information which allows one to interpret geophysical results not in isolation, but in light of historical knowledge. This step typically includes systematic collection and critical review of (i) primary historical sources, such as ancient literary references, inscriptions, and itineraries; (ii) archival and legacy documentation, including early excavation reports, antiquarian notes, drawings, and unpublished field diaries; and (iii) modern secondary sources, such as typological syntheses, regional archeological studies, and previously produced plans or interpretive maps. Even when direct mention of a specific structure is absent, historical sources can provide clues on the functional role of a building within the urban layout, the expected circulation patterns, and the probability of later transformations (e.g., reoccupation, spoliation, or re-planning), which are essential to interpret non-symmetric or multi-phase subsurface evidence.

In parallel, archeologists may leverage comparative analysis of architectural and stratigraphic data (e.g., settlements of similar chronology, administrative status, and urban scale). Such a comparison is performed at two levels. First, at the architectural–typological level, where standard building components, relative proportion of features, and expected spatial sequences (e.g., halls, aisles, annexes, entrances, porticoes, pavement levels) provide plausible templates against which geophysical evidence can be evaluated. Second, at the process-formation level, known patterns of collapse, robbing trenches, and later alterations offer signature examples onto which new observations are compared. This dual comparative approach is especially useful for discriminating features that likely differentiate the original design of a building from those that more plausibly indicate later, site-specific adaptations.

Historical and comparative reasoning also support the explicit treatment of uncertainty in archeological interpretation. Rather than assigning a unique interpretation to a geophysical anomaly, archeologists often develop a set of ranked hypotheses that reflect multiple scenarios consistent with the evidence (e.g., "wall line vs. rubble concentration vs. resurfacing episode"). These hypotheses are then tested against independent constraints: geometric consistency across the dataset, expected construction logic derived from typological parallels, and compatibility with documented historical phases of the settlement. In this framework, the absence of symmetry is not treated as an anomaly per se, but as a potential indicator of diachronic change, such as phased extensions, partial rebuilding after damage, or functional reconfiguration—patterns frequently documented in long-lived Roman urban contexts.

2.3. Leveraging Geomatics for the 3D Reconstruction of Architectural Elements

The geomatic survey is a central component of the methodological workflow, as it generates the spatial and metric basis for the reconstruction of ancient structures. In this study, Close-Range Photogrammetry was used in order to obtain high-resolution three-dimensional data of the visible architectural remains. Several photogrammetric acquisitions were performed using high-resolution cameras mounted on a UAV platform. The images acquired in continuous mode during the flight are then processed using the Structure-from-Motion (SfM) and the Multi-View Stereo (MVS) strategies [19]. These generate dense, textured 3D point clouds and a high-resolution orthophoto, suitable for subsequent interpretation and analysis in a CAD environment. Data acquisition is then followed by the 3D reconstruction phase, which eventually results in the hypothetical configuration of the original ancient structures. This phase consists of analyzing the alignment of the walls, considering the construction technique and architectural proportions highlighted by the model, including and verifying the correspondence with historical

documentation, including items from excavation records, and taking into consideration architectural typologies. The reconstruction process was not limited to the construction of a mere geometric model. Indeed, by integrating the aforementioned aspects, it became an evidence-based interpretative tool for inspecting the site's spatial organization and architectural evolution. Once the plan of the area was obtained, the first step was to build 2D vector representations of each masonry partition, including building elevations. This allowed us to create an accurate and reliable representation of the current state of the site. In addition, the CAD-based representation allowed for a preliminary analysis of the genesis of the structures emerging from the ground and enabled the investigation of symmetry and respective alignment of the various structures comprising the archeological site. The CAD representation is the foundational step toward a complete 3D reconstruction. As such, it must be accurate and detailed. The phase following the two-dimensional drawing is the transition to 3D modeling, whose final product is, in turn, a virtual architectural model (VAM). The latter is achieved by leveraging task-specific software such as Rhinoceros (Versione 8 SR9), which can produce models of the objects present in the archeological area. The purpose of this task is to augment the plan drawing by integrating the full extent of the data obtained from the 3D survey, particularly concerning the extraction of the height of each individual element. The latter consists of extruding closed-base polygons to the chosen heights and converting the resulting wireframe structures into solids, which are then textured or further edited.

2.4. Geophysics Survey

Geomatic methods are extremely powerful in collecting and recording the spatial distribution of present-day evidence and therefore, in providing a virtual representation of visible features. As such, they provide a comprehensive and browsable perspective of the archeological site, offering a view of the "bigger picture" that surpasses what can be obtained through just field observations. On the other hand, the role of applied geophysics is to investigate the subsurface to locate or identify, in a non-invasive way, those volumes of archeological interest that will eventually become targets for future excavations. From a geophysical standpoint, our workflow starts from acquiring and processing a set of raw radargrams (i.e., B-scans) and extracting from these a set of robust, spatially constrained volumes indicating, within a reasonable approximation, the location of the bodies responsible for the observed radar reflections. The classic approach to achieve this goal is to acquire the scans along the lines of a regular grid, ideally oriented so to ensure that the lines cross over the expected features (e.g., walls). Each raw profile is then processed to make reflection events stand out as much as possible. Standardly, processing includes time-zero correction, *dewow*, band-pass filtering, suppression of laterally coherent noise (background removal), and amplitude compensation (e.g., SEC/AGC or equivalent) to mitigate depth-dependent attenuation, which is especially critical in conductive soils. Two-way travel-time is then converted to depth by estimating EM wave velocity directly from the dataset (typically through diffraction hyperbola fitting), thus providing a metric scale for reflector geometry. A data volume is usually produced by interpolating the B-scans. Additionally, each column of the volume is shifted vertically to account for elevation. Finally, the volume is sliced at variable depths, to intercept structures of interest such as walls or similar archeological evidence, obtaining the so-called C-scans.

However, depth slices require dense and regularly spaced profile grids to avoid interpolation artifacts. While interpolation is still possible for sufficiently dense non-regular grids, when acquisition geometry is irregular or coverage incomplete, the interpolation required to generate a 3D grid may introduce significant artifacts. Our dataset consisted of irregularly distributed B-scans with variable spacing and orientation. Additionally,

differences in length of the swaths caused gaps in parts of the area. Interpolation in such conditions would lead to significant artifacts in the C-scans. For this reason, interpretation may rely directly on georeferenced radar profiles rather than interpolated volumes. As such, we adopted a visualization-based approach in which individual radar profiles were georeferenced, positioned in a 3D space, and corrected using the high-resolution DSM obtained from UAV photogrammetry. This approach allowed us to maintain the original spatial integrity of the measurements while enabling cross-comparison between intersecting and adjacent profiles. The rationale we followed for volume extraction is that anomalies are required to show lateral persistence across adjacent profiles and geometric consistency at line crossings, must be observed at consistent depths, and must be clearly visible in all frequency regimes allowed by the antenna (accounting for expected resolution and penetration differences).

Anomalies meeting these criteria were finally summarized as volumes of interest, i.e., 3D spatial entities delineating the extent of organized back-scattered energy, or representative of the approximate location of the scattering body. We represented such VOIs as ranked by confidence, based on reflection strength, spatial continuity, and multi-profile support. Consequently, the processing and interpretation of the dataset involved four main phases:

1. Processing of the 2D scans;
2. Building a 3D assembled view of the GPR scans;
3. Interpretation of the scans by cross-comparing the visible anomalies and extraction of volumes of interest (VOI);
4. Comparison of the VOI with the virtual architectural model (VAM) and further refinement and/or interpretation.

Each phase entailed several lower-level tasks as detailed by the scheme in Figure 2.

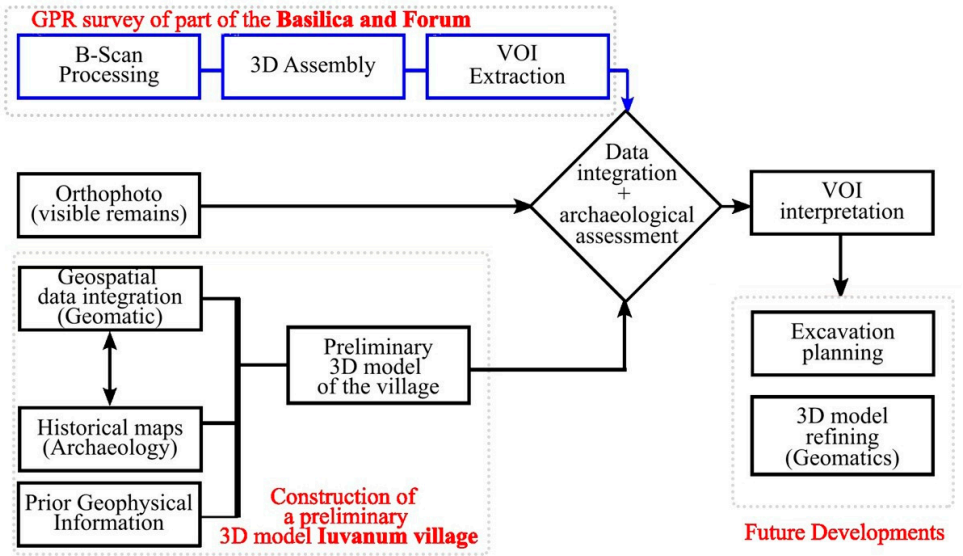


Figure 2. Conceptual flowchart showing the main processing steps and the contribution of different disciplines to the present study. A preliminary virtual architectural model of the entire Iuvanum settlement was generated early in this research, based on geomatic and archeological considerations and incorporating all prior information (including an electromagnetic survey). Geophysics, through the use of GPR, was later leveraged to investigate the subsurface beneath a portion of the basilica and the forum that had not previously been included in any survey, in order to improve the available information. All results were integrated into a comprehensive 3D representation and critically evaluated. The outcome of this process is the planning of new excavations, which will eventually lead to a further improved 3D model.

The black branch shows the contribution of geomatic disciplines that, combining field measurements and archeological knowledge, produced a comprehensive three-dimensional virtual architectural model (VAM) of the entire town of Iuvanum, including terrain, roads and buildings. The blue branch shows the contribution of geophysics through the use of GPR for the investigation of a portion of the basilica building and the forum. The contributions from the different disciplines eventually merge into a multi-perspective, multidisciplinary assessment of the evidence. In particular, the VOIs obtained from the GPR survey for these structures (basilica and forum) are compared with the corresponding portion of the larger (preliminary) VAM, which already incorporates previous knowledge. The VOIs are therefore interpreted from an archeological perspective both to plan new excavations and to refine the architectural model where necessary. The GPR investigation was conducted without prior knowledge of subsurface structures, the architectural model or any other information, to ensure an unbiased identification of anomalous features. Subsequently, the three-dimensional representation comprising radar scans and VOIs was combined with the model of the town and the terrain surface (textured with the orthophoto) to build a comprehensive representation. This new virtual representation constitutes a very powerful tool which enabled our archeologists to formulate several hypotheses and plan future excavations.

3. Case Study

3.1. Brief History and Identification of the Area of Interest

The archeological site of Iuvanum is located on a hilltop in the Abruzzo region of Central Italy, between the modern municipalities of Montenerodomo and Torricella Peligna. The settlement represents a significant case study for investigating the transition from Samnite to Roman urban organization in the central Apennines [20–22]. The earliest occupation of the area dates to the Samnite period, when the territory was inhabited by the Carricini tribe [23,24]. Archeological evidence suggests that a small settlement developed around a pre-Roman sanctuary, which functioned as a focal point for religious and commercial activities [25]. The lower plateau hosted an early market area that initially operated as a forum boarium and later acquired broader civic and political functions. Between the 2nd and 1st centuries BC, following the progressive consolidation of Roman influence in the region, the settlement evolved into a forum vicus characterized by an increasingly structured civic and commercial organization. During this phase, particularly between the end of the 1st century BC and the first half of the 1st century AD, the urban layout was reorganized according to Roman planning principles. Public spaces were monumentalized through the paving of the forum, the construction of a large basilica, and the development of rows of *tabernae* along the edges of the square, forming the architectural framework of the civic center. The archeological area and the main visible monuments are illustrated in Figure 3b. The area of interest (AOI) covered by the study encompasses part of the forum and part of the basilica, as indicated in Figure 3c,d, corresponding to the central sector of the Roman civic complex. From a functional perspective, this sector likely represented a zone of intense circulation and interaction between administrative, commercial, and public activities. The area may have hosted connective and service structures, including porticoed corridors, thresholds, stairways, internal partitions, and ancillary rooms associated with the surrounding public buildings and the *tabernae* facing the forum. Many of these architectural elements were constructed using relatively light techniques or were repeatedly modified during successive occupation phases. In addition, systematic stone robbing and post-abandonment reuse have significantly reduced their surface visibility. Nevertheless, such structures may still produce detectable subsurface signatures, including foundation remains, construction trenches, and robbed-wall features.

Furthermore, interstitial spaces between major public buildings frequently accommodated infrastructural systems related to water management and drainage, such as channels, culverts, and sewer lines. Although these installations are rarely visible today, they can persist as subsurface anomalies detectable through non-invasive geophysical and remote sensing methods. The investigation of this sector therefore offers the potential to reconstruct the internal organization and architectural evolution of the forum area, contributing to a better understanding of the spatial configuration of the Roman civic center at Iuvanum.

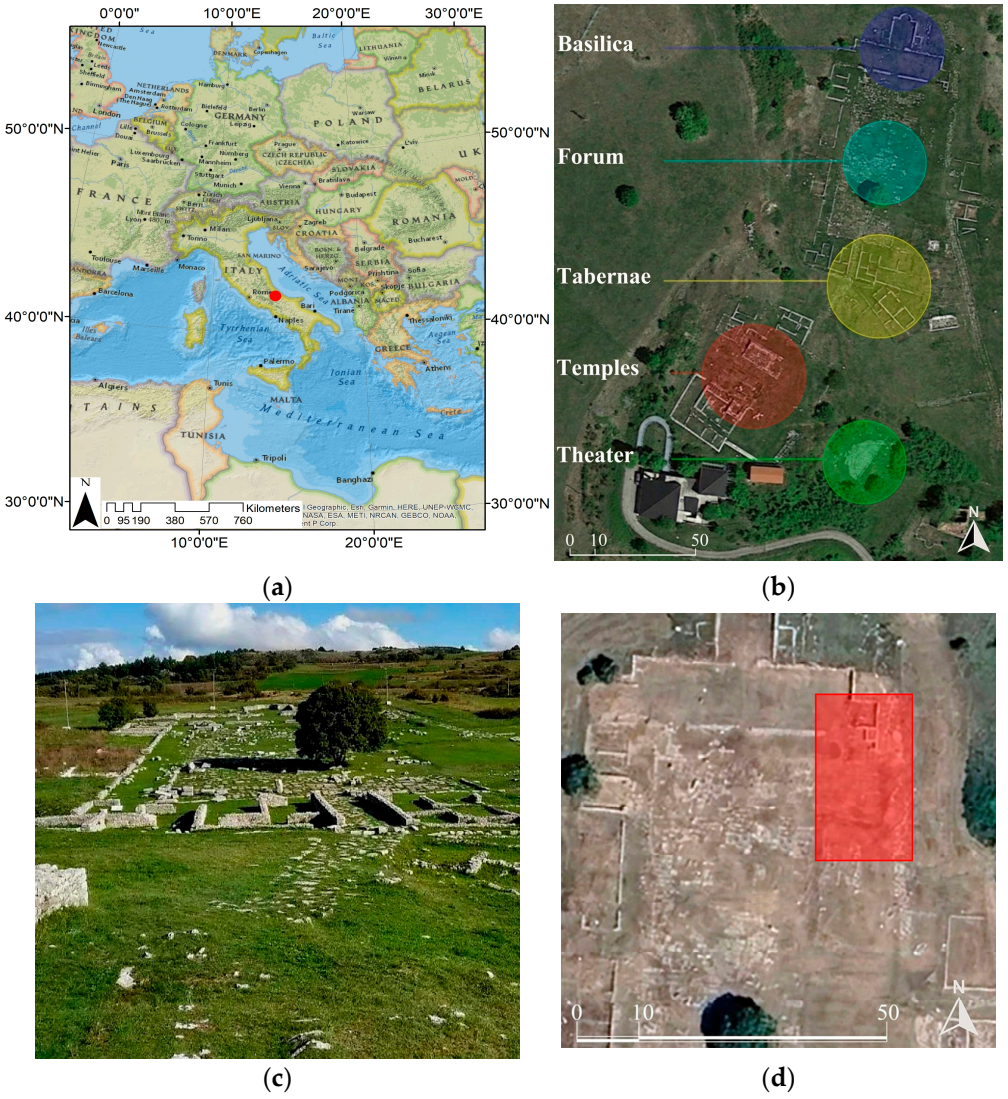


Figure 3. Case study framing: (**a**) geographical location, (**b**) identification of the main structures, (**c**) panoramic photo and (**d**) area of interest on the Google Earth basemap.

3.2. 3D Survey

The photogrammetric survey was carried out using a DJI Mavic 4 Pro (DJI, Shenzhen, China), unmanned aerial vehicle (UAV), selected for its versatility, stability, and high imaging performance. The DJI Mavic 4 Pro is a compact multirotor UAV equipped with a triple-camera system. Its main Hasselblad camera incorporates a 4/3 CMOS sensor with 100 MP effective resolution and supports image acquisition in JPEG and DNG (RAW) formats, with a maximum image size of 12,288 × 8192 pixels. The acquisition flight was performed manually, allowing the operator to adapt the trajectory dynamically to the topographic and architectural characteristics of the study area, which included the forum and the basilica. Despite the absence of a predefined flight plan, the image acquisition

followed a systematic approach, maintaining high overlap and sidelap to ensure reliable 3D reconstruction. To capture the full complexity of the site, the survey combined nadiral photographs, taken with the camera oriented vertically, and oblique images, obtained by tilting the main camera by 45°. This strategy is essential for documenting the vertical façades and architectural elevations that would otherwise be partially hidden in nadiral-only datasets. The combination of both perspectives yielded a rich, redundant dataset that covered the entire area of interest, minimizing occlusions and enhancing the representation of vertical and undercut surfaces. The flight altitude ranged between (25–40 m Average Ground Level—AGL), yielding an average Ground Sampling Distance (GSD) of approximately 1.5 cm. For georeferencing, the survey was supported by GNSS measurements acquired with an Emlid Reach RS3 receiver operating in Network Real-Time Kinematic (NRTK) mode. The system provided centimeter-level accuracy in real time, connecting via the cellular network to the regional GNSS correction service. Several Ground Control Points (GCPs) were strategically marked across the survey area prior to the UAV flight, and their location recorded in RDN2008/UTM zone 33N-EPSG:7792 coordinates. The photogrammetric process was carried out using Agisoft Metashape Professional, employing a SfM and MVS workflow leveraging pipeline processing comprising the following steps [26,27]: (i) image alignment and sparse point cloud generation; (ii) camera calibration and bundle adjustment, refined through optimization of internal and external orientation parameters; (iii) dense point cloud generation; (iv) mesh model creation and texture mapping, to produce a geometrically consistent and visually realistic 3D representation; (v) and generation of the orthomosaic and the digital surface model (DSM).

The high-resolution digital elevation model (5 cm/pixel) accurately represents the morphology of the Iuvanum site, allowing for clear distinction between archeological structures and the main topographical variations in the area (Figure 4).

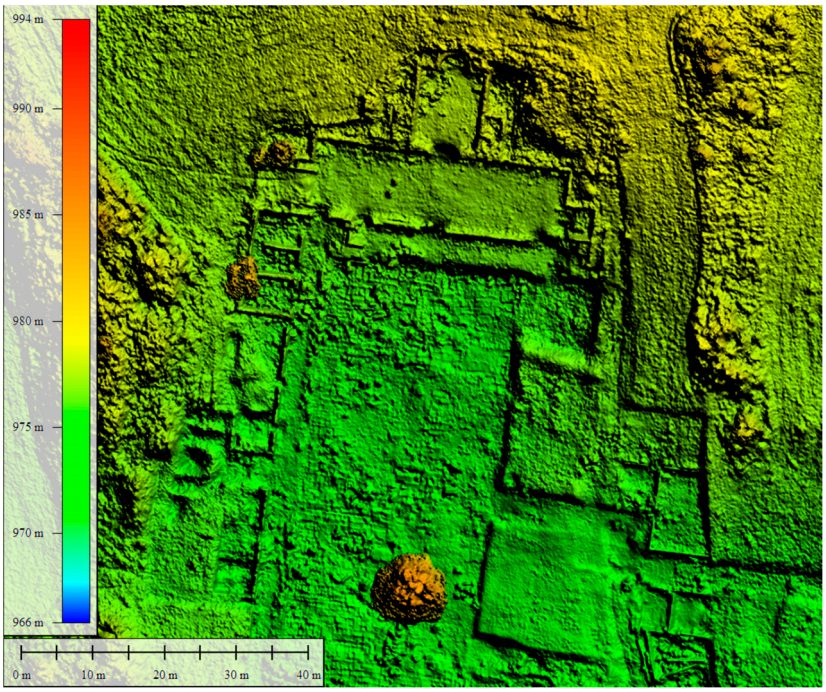


Figure 4. DSM of the archeological site of Iuvanum; the minimum elevation is 974 m and the maximum elevation is 977 m.

The integration of oblique and nadiral imagery, combined with the high optical performance of the Mavic 4 Pro, produced a detailed and metrically accurate 3D representation of the forum and basilica area. The resulting dataset not only documents the site with

an extraordinary level of detail but also demonstrates the effectiveness of manual UAV photogrammetry as a flexible and reliable method for surveying complex archeological environments [28]. Figure 5 shows a view of the obtained point cloud.



Figure 5. View of a portion of the 3D point cloud obtained for the Iuvanum site. Specifically, the image shows the northern portion of the basilica, where the GPR survey discussed in the following sections was performed.

3.3. 3D Modeling and Reconstruction

The process of three-dimensional modeling and reconstruction of the Iuvanum site is an essential part of an integrated workflow that transforms raw numerical data into a semantic model with high information content. The geomatic survey described above has generated a multidimensional dataset with high geometric accuracy and detail, which provides a reliable metric framework for any subsequent reconstructive deduction. This digital documentation should be considered as a dynamic and searchable three-dimensional archive, in which morphological features of each individual archeological remain are captured and digitally preserved. The transformation from point cloud to a solid geometric model required a rigorous analytical methodology.

First, efficient management of such a dense point cloud requires extracting appropriate planar sections and converting in raster format the points belonging within each section. This strategy allowed us to reduce the amount of data and employ less memory resources. This task was achieved using the software PointCab (Origins 4.2). This phase was also critical for judging the symmetry of the basilica and comparing the current state with the historical documentation. At this stage, the orthophotos produced (Figure 6a) were systematically overlaid with the plans of the areas excavated during earlier campaigns (Figure 6b) in order to identify visible features that had symmetrical counterparts in the already excavated sectors.

This provided a solid basis for the subsequent work of connecting the above-ground and underground structures.

The next step of the workflow, the vectorization phase, was performed in AutoCAD (2025) software. This task was not a mere graphic tracing exercise but entailed an in-depth interaction with our archeology experts to make sure that every detail of the geometric interpretation was accurate from a historical and archeological perspective. Vectorisation of a complex archeological site such as Iuvanum entails dealing with remains of structures built in different epochs, where the geometry of walls changed as the buildings underwent structural remodeling or changed destination of use. This critical analysis allowed us to

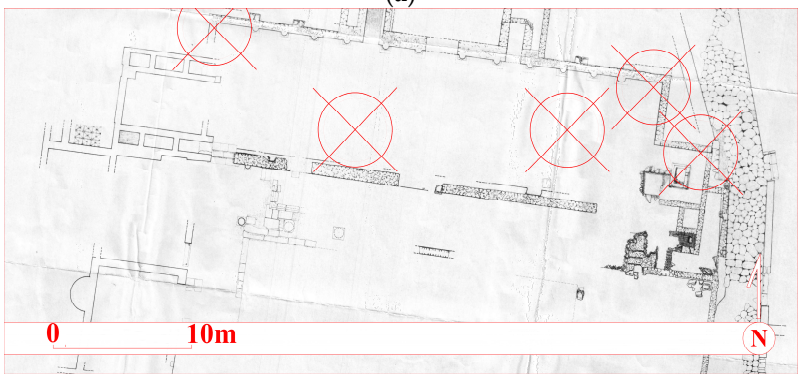
isolate the forum's vector "skeleton" and ensure that the subsequent volumetric model was not merely an ideal reconstruction, but a coherent reflection of the construction logic of antiquity. The main challenge was the extreme incompleteness of out-of-the-ground remains, often limited to a few rows of masonry blocks, insufficient both to deduce the original height or the development of the architectural orders. In this fragmentary state, we may recognize one of the limitations and main challenges of our work, as it is impossible to restore what time has eroded. To fill the gap, we adopted an approach based on metric and proportions. Specifically, drawing on architectural canons and based on the symmetry parameters found in the surviving portions of the basilica and forum. Figure 7a shows the three-dimensional modeling of the current state, where existing wall partitions are modeled and the axis of symmetry of the forum is traced in red. Observing the surviving wall segments in situ, the basic construction modules and planimetric guidelines were extracted. Knowledge of these elements guided us in the development of the model towards those areas where visible clues are absent or unexcavated. The choice of a symmetric configuration with respect to the main axis (Figure 7) is not an arbitrary choice, but the result of cross-comparing the distribution of the archeological remains throughout the site, which are clearly disseminated symmetrically with respect to the basilica central axis. The digital reconstruction allowed us to further confirm that this symmetry hypothesis was indeed well justified as it explained most of the residual traces on the ground. The reference to symmetry in this study does not imply a perfect geometric correspondence among all the architectural elements visible in the orthophoto. As clearly observable in the orthophoto itself, the sides of the basilica and the shorter side of the forum are not strictly symmetrical. These deviations represent important archeological evidence and reflect the complexity of the built environment. In this context, the concept of symmetry refers primarily to the main architectural axis connecting the basilica and the forum, oriented along the north-east/south-west direction. Such axial relationships represent a recurrent planning principle in Roman public architecture and appear to structure the spatial organization of the civic complex. The symmetry considered in the interpretative reconstruction therefore concerns the basilica, the forum square, and the portico surrounding the forum, which seem to follow this axial arrangement. In contrast, this principle does not extend to the *tabernae*, whose layout presents clear irregularities and local adaptations, as also documented by the orthophoto. Figure 7b shows the final three-dimensional rendering of the forum created by leveraging this symmetry assumption.

The resulting model is not to be considered a final reconstruction of the forum, nor it is the only possible appearance that this place displayed back in time, but rather a 3D interpretation of the forum on which all known information and available evidence are converged. Wherever information is missing, undocumented areas were inferred from the recorded elements and checked against the surrounding topography. This process required a continuous interplay between the reconstruction design and the point cloud, to ensure that each newly added geometric element was compatible with the existing evidence and when the cases constituted a harmonic architectural continuation, they were added to the reconstructed picture. Figure 8a shows an axonometric view of the point cloud while Figure 8b shows the overlap between the point cloud (actual state) and the reconstructed three-dimensional model. After the vectorization and the critical interpretation phase, we proceeded to the volumetric extrusion which transformed the interpreted plans into the final solid 3D model necessary for rendering and visualization. This latter process was performed by importing the 2D plan of the entire complex into the Twinmotion environment, where proper material attributes were assigned to each object in the scene. To generate a realistic physical and chromatic appearance of the ancient surfaces, building materials and consequently texture and graphical properties were decided on according to

the building criteria of the time, and archeological evidence. In particular, to render the variations in the plaster and flooring, we selected material properties that reproduced the appearance of local stone, the main construction material found on the site.



(**a**)

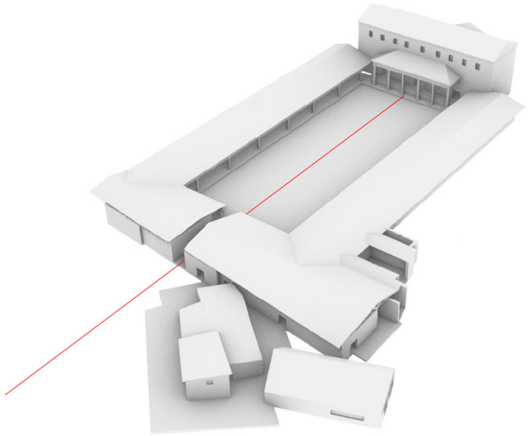


(**b**)

Figure 6. Comparison between maps generated by different approaches and in different periods. The same portion of the northern part of the forum and the basilica are shown. (**a**) Orthophoto generated using our geomatic approach (see Section 3.3 and the following sections). The image captures not only geometry, but also visual details related to the different levels of preservation of the remaining walls. Control points are highlighted in yellow. (**b**) Planimetry from archive documents from a survey and excavation dated back to 1988. Control points are highlighted in red.



(**a**)

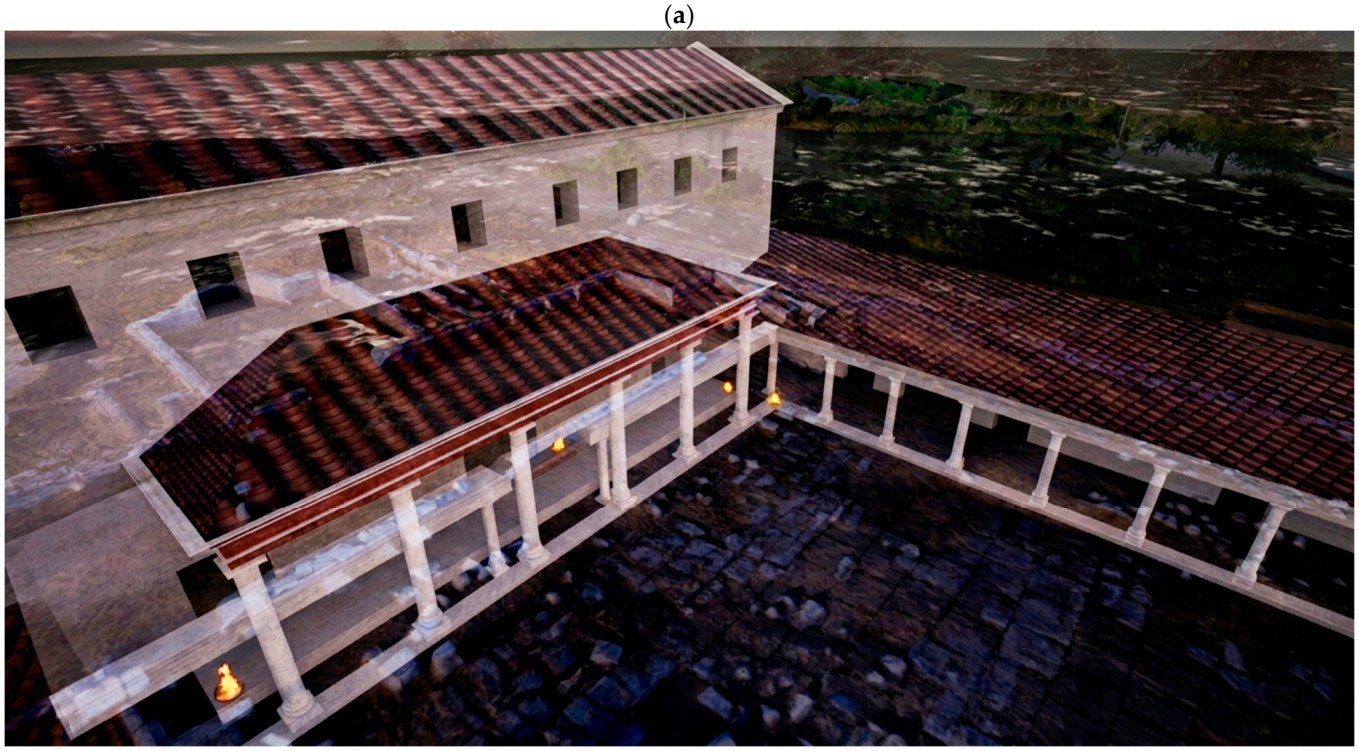


(**b**)

Figure 7. Reconstruction of the structures: (**a**) identification of an axis on orthophoto and (**b**) reconstructed 3D model. The red line represents the main symmetry axis of the structure.



(**a**)



(**b**)

Figure 8. Axonometric view of the reconstructed part of the archeological site in its current state: (**a**) point cloud and (**b**) overlay between 3D model and point cloud.

Special attention was also devoted to the reconstruction of the surrounding environment, integrating the terrain data to recreate the complex orography of the Iuvanum site in an accurate way. Further inclusion of graphical details such as vegetation and terrain texture allowed us to take a step further, imaging the Iuvanum site as it would have probably appeared to its inhabitants. Indeed, the rationale behind this final effort was to produce an evocative reconstruction intended to support public outreach. Nevertheless, placing the architecture within such a plausible context allowed us to judge whether the model conveys the correct perception of the relationship between the built environment and the natural space.

The suggestive view offered by the photorealistic rendering in Figure 9, therefore, is not only a striking esthetic communication tool, but also serves as a fundamental verification tool, allowing the architectural coherence, visual impact and validity of the reconstruction hypotheses to be assessed.

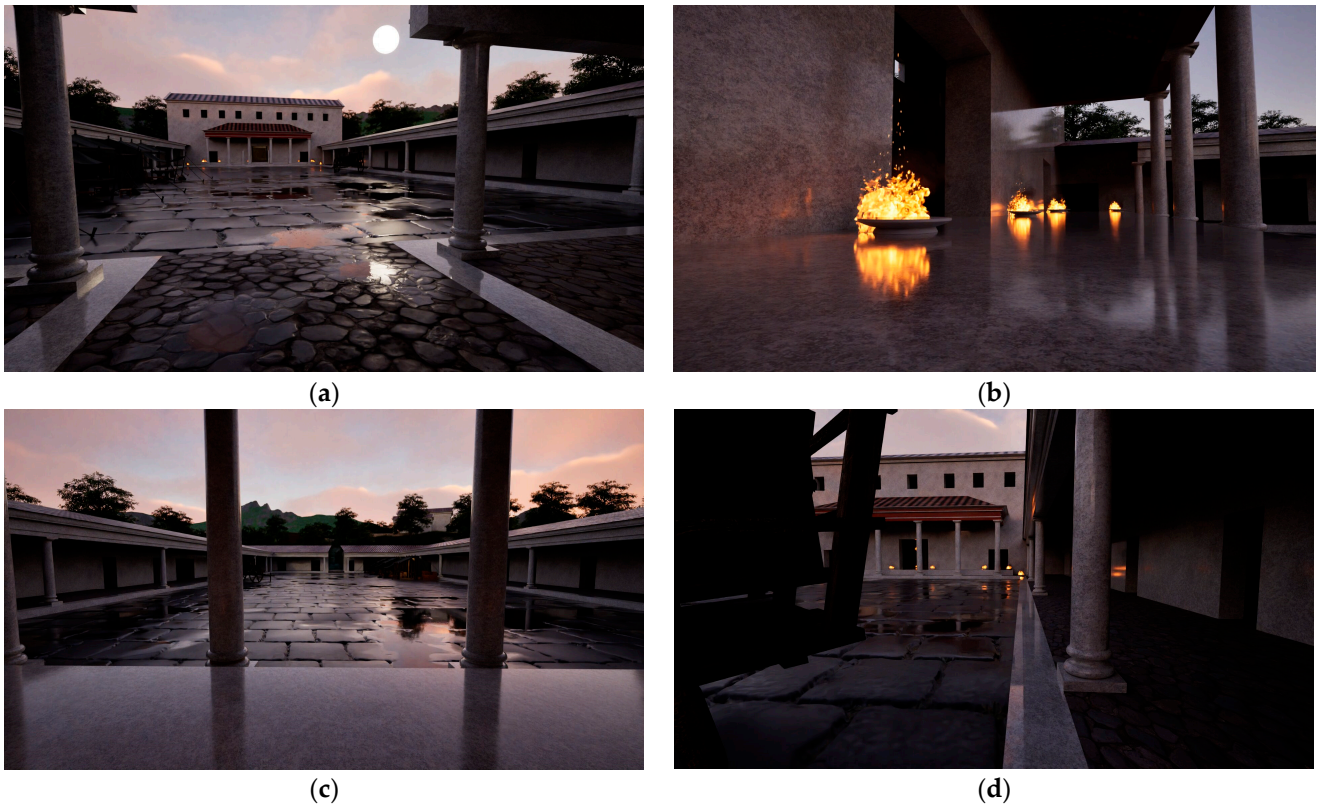


Figure 9. Textured three-dimensional model rendering of the Iuvanum: (**a**) view of the forum from the entrance, (**b**,**c**) portico of the basilica and (**d**) side portico.

The renderings shown in Figure 9 represent a 3D reconstruction of the basilica and forum of Iuvanum developed according to a "data-driven" approach, in which formal choices are anchored, as far as possible, to archeological evidence, surveys/orthophotos, and bibliographic sources integrating, where necessary, the results and conventions already used in the previous virtual reconstruction 2008–2011. The result is a model that favors metric and constructive consistency, making explicit the transition from observable data to the hypotheses necessary to complete the elevations and roofs. Methodologically, the reconstruction proceeds by progressive constraints. First, a hierarchy of quotas is defined starting from the plan of the square and the recognizable differences in height (e.g., steps and access levels also visible in orthophotos), in order to establish the layout of the porticoes and the elevation of the basilica above the forum. Secondly, the geometry of the porticoes is reconstructed using a modular criterion based on the number of supports and the inter-axes documented/reconstructed in the literature; the rendering of the columns (including the corner ones) also incorporates principles of perceptual correction referred to in the sources. Finally, the elements for which direct measurements are available (e.g., shafts and bases in situ) are taken as dimensional anchors, while the missing parts (overall height, tapering, entablatures) are derived using proportional rules typical of the order and with checks for consistency with the portico system. For the basilica, the model interprets the building as a large unified space overlooking the forum, with the internal structure divided by the half-columns preserved on the northern side. The distribution of the upper openings is reconstructed according to the compositional logic imposed by this internal rhythm.

The choices relating to the superstructure (attic with windows/clerestory) and the roof (wooden trusses with coffered intrados) are justified in the dossier with reference to both structural considerations (compatibility with wall thicknesses) and typological comparisons with basilicas in smaller towns; where evidence is insufficient, alternative interpretations (e.g., for the entablature) are explained, supported by external comparisons. The apsidal space behind, interpreted as an Augusteum/tribunal, is reconstructed with a distinct spatial hierarchy also in terms of height and treatment, consistent with the functional centrality attributed to it by sources and with reference to the epigraphic evidence. The characterization of materials follows the same criterion: where evidence is direct (e.g., local limestone paving in the square, with recesses for bronze letters; tuff half-columns with plaster; marble flooring of the Augusteum), the model adopts materials consistent with the descriptions; where the data are indirect (e.g., flooring of the basilica), a plausible proposal is used, deduced from excavation reports and functional analogies, keeping the "documentary" component separate from the interpretative one.

3.4. Preliminary Geophysical Test (GPR)

Ancient Roman structures are characterized by a high degree of symmetry. As such, it could be expected the basilica building had to be symmetrical with respect to its central axis, with the east section mirroring the west, excavated side. Yet some asymmetric features in the visible remaining structures suggest that additional, and most importantly, non-symmetrical elements were present.

Based on these considerations, we leveraged the ground-penetrating radar to investigate part of the north-eastern portion of the basilica (Figure 3d), not covered by any previous geophysical investigation. The purpose of this survey was twofold: on the one hand, we aimed at establishing whether buried structures in a configuration symmetrical with respect to known architectural elements could be observed. On the other hand, we wanted to explore to what extent the asymmetrical elements, still visible, were just of secondary importance or rather symptoms of a greater deviance of the ancient building from the hypothesized symmetric structure.

The GPR acquisition was performed leveraging an IDS Georadar Hi-Mod System (IDS GeoRadar, Pisa, Italy) equipped with a dual-frequency antenna of 400–900 MHz.

In the beginning, we planned a classic grid survey, with radar swaths performed along two sets of mutually perpendicular lines, with a 1 m spacing in both directions. However, what seemed simple in the planning phase had to be changed during practical execution. Despite the relatively small size of the area, the survey comprised three different flat portions of terrain, joined by sloping transition that could change the elevation of the ground (sometime up to 50 cm), over very short distances, causing difficulty in keeping the antenna stable while recording. Additionally, piles of loose stones and remains of ancient walls forced deviations from the ideal grid and required survey lines of variable length. It soon became clear that a traditional grid was simply not feasible, and we were forced to acquire the scans wherever it was convenient. However, even though we could not follow a regular, perpendicular pattern, we still managed to acquire the swats along straight lines whose endpoints coordinates were acquired using a Emlid Reach RS + 3 GNSS. A total of 24 lines were acquired, 16 approximately oriented in the north–south direction, and 8 in the east–west direction, covering an area of 10 by 27 m. The GPR acquisition lasted approximately 3 h. Figure 10 shows an aerial view of the lines with a portion of the local DEM in the background.

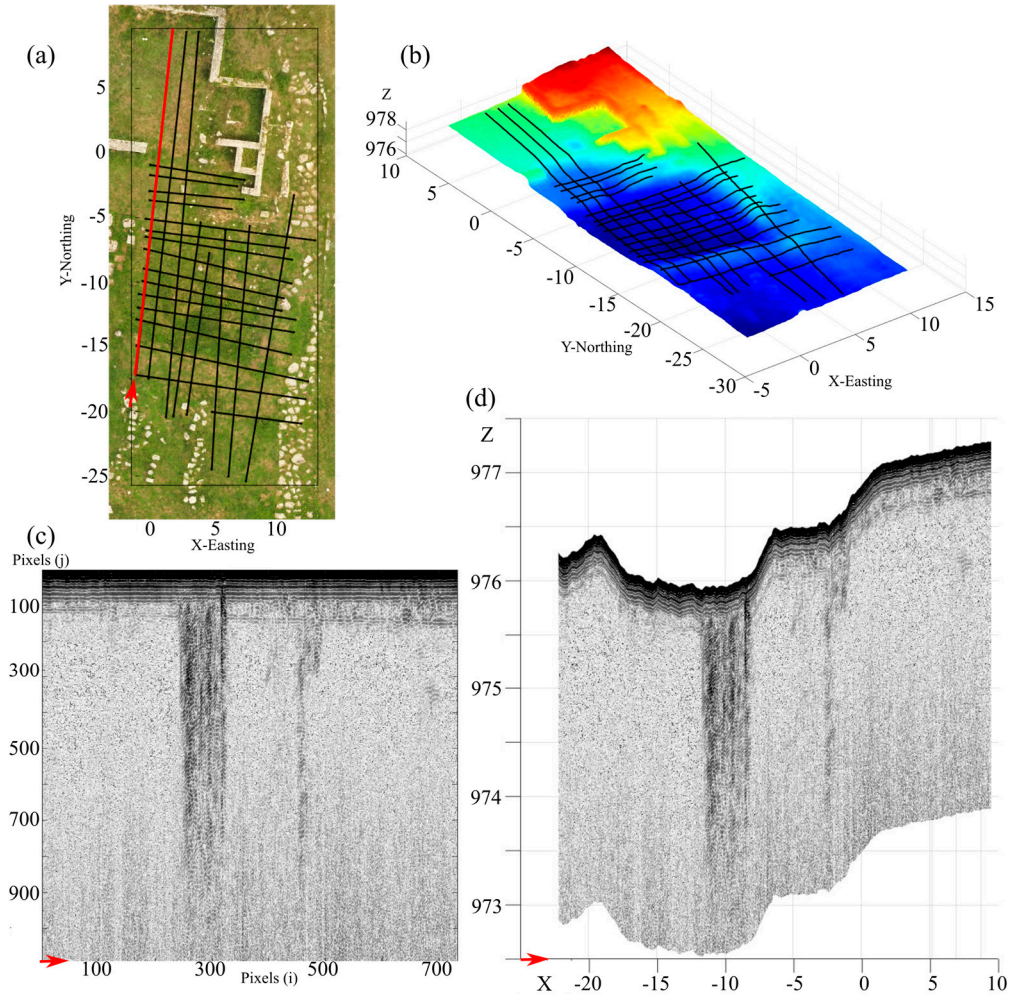


Figure 10. (**a**) Aerial view of GPR acquisition paths. For simplicity of representation, a local Cartesian reference system has been defined, with its origin at the UTM coordinates (437,891.566, 4,649,894.976). The orthophoto of this portion of the basilica and the forum investigated is shown in the background. (**b**) The real-word locations of each pixel column of the B-scans are shown in black and superimposed to the DEM. These lines correspond to the physical location of the radar antenna during the acquisition. (**c**) A selected example of radar B-scan, $A(i,j)$; axes are expressed in pixel coordinates (i,j). The image shows line no. 21. (**d**) The same radar image of (**c**), corrected for elevation (figure not to scale). The red arrow in (**a**,**c**,**d**) indicate the direction of the acquisition.

3.5. GPR Scan Processing

Processing of GPR individual B-scans was carried out using the ReflexW software (Sandmeier Scientific Software, Karlsruhe, Germania) [29]. The processing steps, summarized in Table 1 for the two antennas, were tailored on the data to maximize the chance of observing every deep, low amplitude reflection, especially considering the strong attenuation due to the moisty, clayey soil present at the site.

GPR B-scans are complex valued images where each pixel holds the complex amplitude $A(i,j)$ of the back-reflected electromagnetic wave and where the horizontal (i) and vertical (j) positions along the image's edges represent the distance walked on the ground by the antenna and the two-way travel-time of the wave, respectively. The GPR scans were acquired with an along-track sampling step of 1 cm, while the spacing between adjacent swaths varied from 1 m (in most cases) to 2 m, delineating a set of irregular trapezoidal zones (Figure 10a). However, since scans had different lengths, the grid presented several gaps.

Table 1. GPR data processing parameters.

Type of Antenna	
Antenna 1 (A1), 900 MHz	*Antenna 2 (A2), 400 MHz*
Butterworth bandpass filter, 600–950 Mhz	Butterworth bandpass filter 200–550 Mhz
Correct the maximum phase, according to the positive polarity in the time-window 7–12 ns.	Correct the maximum phase, according to the positive polarity in the time window 5–15 ns.
Move start time	Move start time
Custom gain function.	Linear gain after 10 ns, 1 db/m
Background removal	Background removal
Subtract mean (dewow), time-window: 10 ns	Time cut at 100 ns
Time cut at 80 ns	

Our site comprises ancient wall remains (our target) built with local rocks and mortar, embedded in a humid, clayey soil matrix. On the one hand, we could rely on the strong contrast between the target material and the embedding soil. On the other hand, the radar signal is known to suffer strong attenuation in this kind of soil, resulting in a severely reduced depth of investigation. As such, to at least partially compensate for the loss of signal amplitude, we found it extremely useful to visualize the data in terms of amplitude on a logarithmic scale.

3.6. 3D Assembly

Assembly of the radar swaths into a 3D representation was achieved by a two-step process. First, we needed to obtain the three-dimensional (i.e., real-world) representation of all B-scans. To do so, we developed a script in Matlab R2024b to perform the following operations: (1) load all traces; (2) convert the two-way travel-time into depth, using the estimated velocity of the electro-magnetic signal in the soil (8.5 cm/ns) estimated from observing the diffraction hyperbolas present in the data; (3) using the GPS locations of the scans end-points, compute the (x_c, y_c) position in the real world of each column of pixels of the image; and (4) compute the elevation z of each pixel by extracting the soil elevation at position (x_c, y_c) from the DEM, and subtract the estimated depth of the pixel. Figure 10 depicts a few milestones of this process. Figure 10a shows an aerial view of the straight-line GPR acquisition paths. The background of the image is color-coded according to the elevation of the ground (i.e., according to the DEM).

Figure 10b shows the elevation along the antenna paths after step 3, described above. In this figure, paths are shown in 3D along with a portion of the digital elevation model—DEM (the latter is color-coded using the same scale used in Figure 10a). To estimate the elevation error associated with this interpolation, we computed the vertical distance between the interpolated pixel (column) elevation and elevation of the nearest DEM point, finding that 98.4% of the points have vertical differences smaller than 1 cm, and 99.9% less than 2 cm, with the maximum discrepancy being 3 cm. The result of this process comprised three matrices, $x(i,j)$, $y(i,j)$, $z(i,j)$, mapping the flat B-scan image $A(i,j)$ to the 3D space. Figure 10c shows a selected B-scan example, while Figure 10d shows the same scan once corrected for the elevation (the vertical scale has been exaggerated for visualization purposes).

3.7. VOI Extraction

Finally, the four matrices (x,y,z,A) were converted into a structured squared mesh and saved in a VTK [30] (Visualization ToolKit) format for the last step: assembly and visual-

ization. To perform the latter task, we leveraged the "Paraview"software (Ver. 5.13.3) [31], which allowed us to load all mesh files (one for each of the B-scans) in a unified 3D view, which will be referred hereafter as "Assembled GPR View". This process fully preserved the resolution of the original B-scans, while allowing their visualization (and subsequent cross-comparison) in a full 3D environment.

As we have now achieved a 3D visualization of the GPR products, we could now seek clues on possible buried structures (see, for example, Figure 11a).

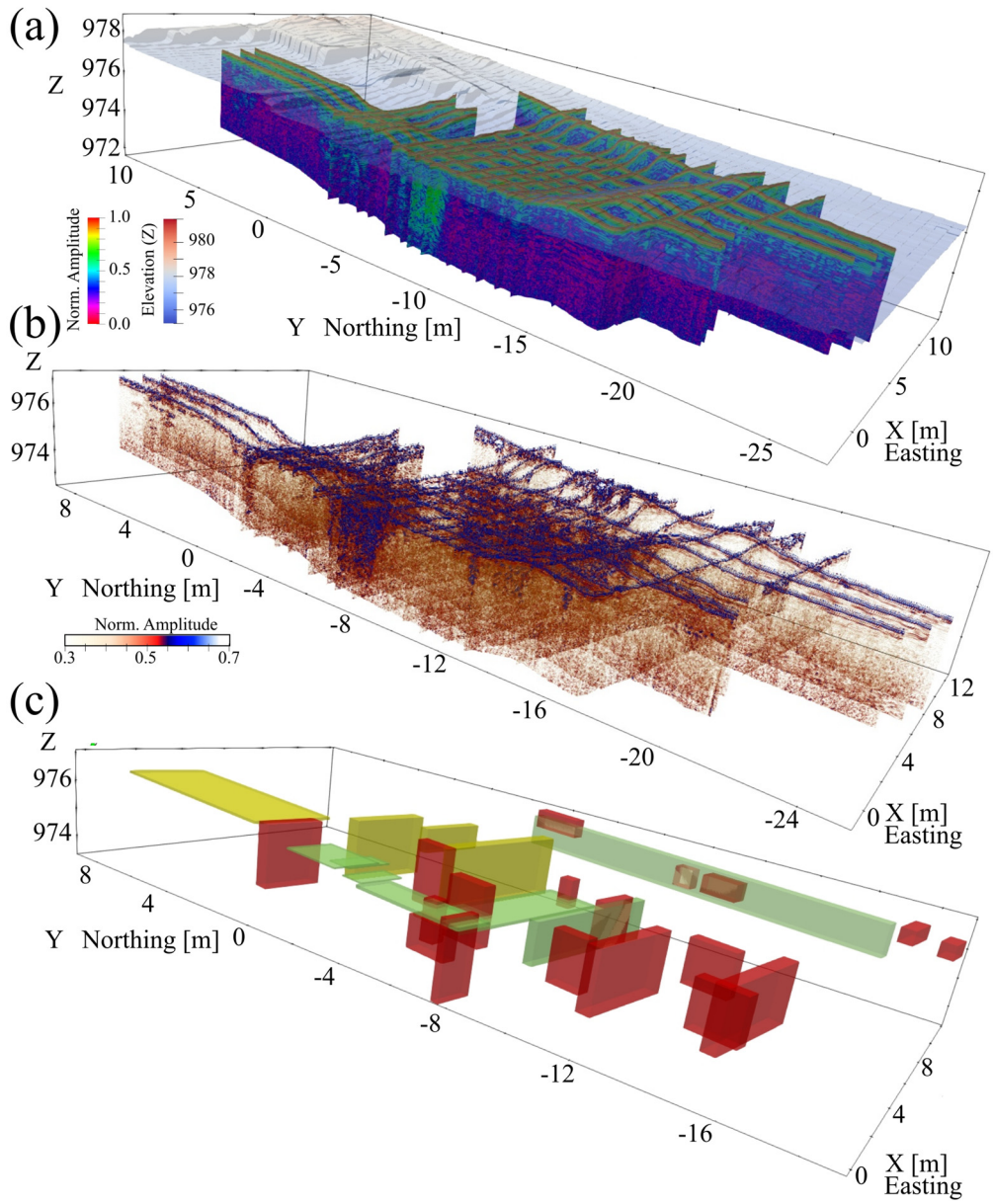


Figure 11. Three-dimensional assembled view of GPR products. Here, the dataset from antenna A1 (900 MHz) is shown. (**a**) Assembled B-scans from antenna A1, with superimposed ground surface (DEM). (**b**) See-through view, highlighting the strongest reflections. (**c**) Volumes of interest extracted from a cross-analysis of the two antennas' datasets.

Specifically, the task consisted of cross-checking different radar scans, in the assembled GPR view, visually comparing parallel scans, seeking common features in the intersecting ones, and comparing features detected by both antenna frequency regimes. Additionally, by leveraging a binary colormap and rendering as partially transparent the portions of the radar images with amplitudes below a suitable threshold, we were able to create a conve-

nient see-trough representation to assess the spatial continuity of the strongest anomalies. Figure 11b provides an example of this representation. The output of this analysis is a set of delineated volumes marking the position and extent of the detected anomalies.

It is important to emphasize that the volumes of interest were not inferred from isolated reflections but were delineated only when anomalies exhibited: (1) lateral continuity across multiple profiles, (2) geometric consistency at line intersections, and (3) coherent depth positioning after velocity estimation and topographic referencing. The delineation of VOIs was performed conservatively and only where coherent reflections were observed in multiple adjacent or intersecting radar profiles at a consistent depth. In addition, they should be interpreted as spatial envelopes summarizing multi-profile reflection patterns rather than volumetric reconstructions of the reflector geometry. A general representation of the reconstructed VOI is shown in Figure 11c, where volumes have been color-coded according to their relevance, as detailed in the Section 4.

3.8. VOI Interpretation

Interpretation of the identified volumes consisted of verifying whether GPR-derived VOIs were consistent with visible remains (when this assessment was possible) and whether the architectural model was compatible with geophysical evidence. This was carried out by overlaying the three-dimensional GPR assembled view with both the DEM, a textured additional surface representing the ground level (textured with the orthophoto), and the entire virtual architectural model of the town, containing the models of individual buildings and their internal walls, as hypothesized. It is worth mentioning that this large, integrated 3D environment has been created to host future GPR surveys that we plan to perform across the Iuvanum site, and more generally to integrate future products from other geophysical approaches. That being said, from now on we will focus exclusively on the north–eastern portion of the basilica.

4. Results

The main products of the present investigation are the 3D integrated representation of geophysical (i.e., GPR) and geomatic products, and the volumes of interest derived from the GPR survey.

The first constitutes a virtual environment in which data of different nature can be merged into a powerful investigation tool. Additionally, the 3D representation can easily import products from different investigation modalities (e.g., magnetic, electric resistivity tomography, etc.). Figures 11–14 were all produced from this virtual environment. Figure 11a,b were produced by turning on only the visualization of GPR products, while in Figure 11c only the visualization of VOIs was activated.

Figures 12–14 present different views of the same volumes of interest with increasing zoom and should be considered in a "large-to-small" perspective.

Figure 12 illustrates the comparison between the interpreted VOIs derived from the GPR dataset and the independently reconstructed three-dimensional architectural model of the basilica (see also Figure 7b). Figure 13 offers a combined view of the 3D building model, VOIs, and the orthophoto. Finally, Figure 14 focuses on volume no. 7 and the B-scans in which the corresponding reflection pattern was observed.

The second product, described hereafter, consists of the volumes of interest derived from the GPR survey. The main goal of any geophysical survey is to detect anomalies within an investigated volume: with GPR, these anomalies are observed through their interaction with the probing electro-magnetic wave and specifically, in form of back-reflected wavelets. As such, radar products are not of immediate interpretation for persons without specialized training. Therefore, since the most probable cause of anomaly in this survey was buried

remains of walls and cluster of collapsed masonry, we deemed it effective to provide our archeologists with a more straightforward representation, through the concept of volumes of interest. This approach is particularly convenient, as it naturally returns valid indications for excavation planning.

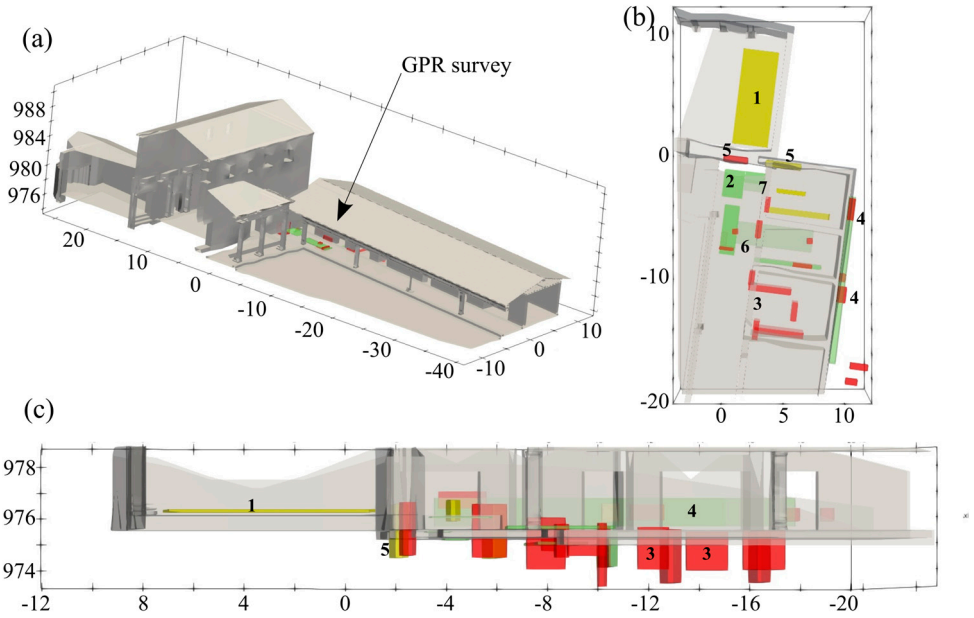


Figure 12. (**a**) Portion of the 3D integrated view showing part of the virtual architectural model (the walls of the basilica), compared to the volumes identified independently leveraging GPR. The two 3D datasets were produced separately and subsequently visualized together to facilitate the archeological interpretation. (**b**,**c**) provide closeup views from the top and the side, respectively. Labels 1–7 identify the volumes discussed in the main body of this article.

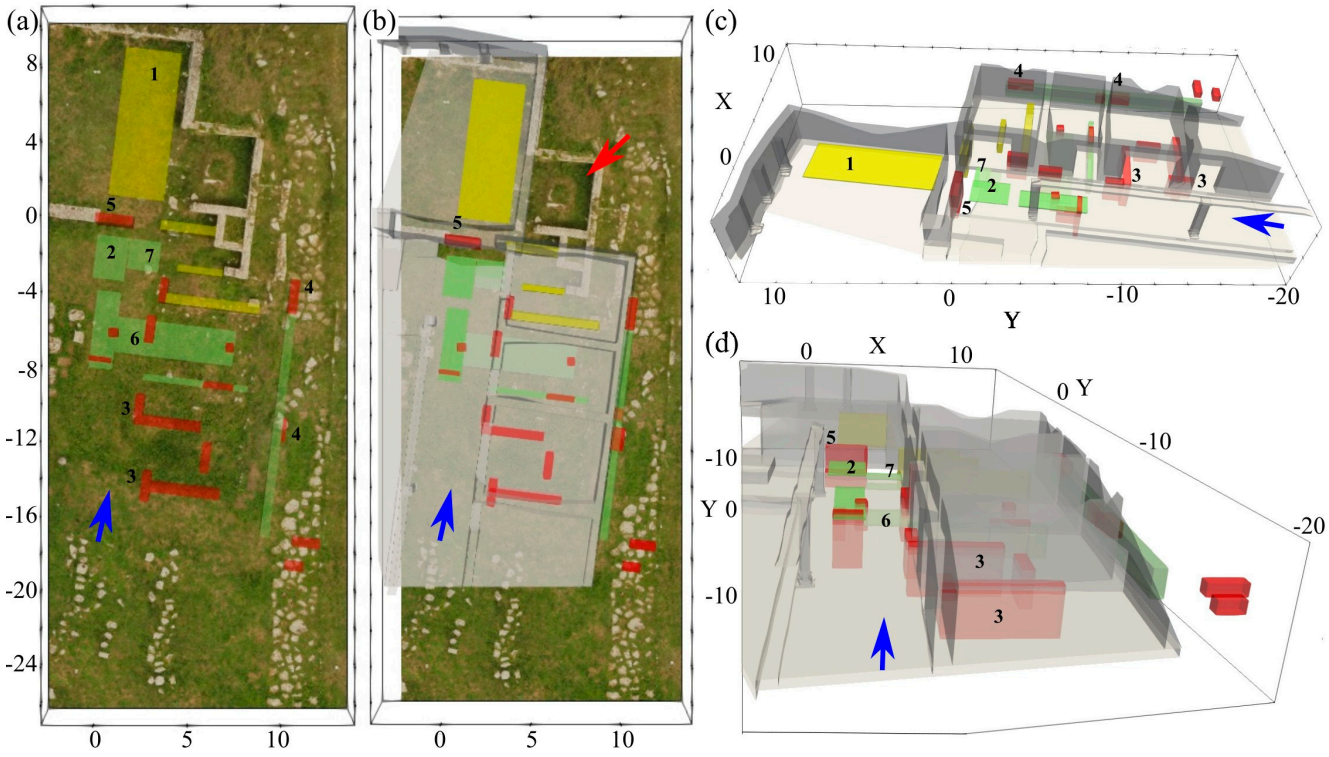


Figure 13. Comparison of geophysical and geomatic results. Labels 1–7 identify the volumes discussed in the main body of this article. The red arrow emphasizes the presence of a non-symmetrical

structure. (**a**) An aerial view of the volumes obtained from GPR are shown overlaid to the orthophoto. (**b**) The same image shown along with a portion of the 3D building model (VAM) overlaid. (**c**,**d**) offer additional views of volumes as compared to the architectural model. The blue arrows indicate the same viewing direction across the figures.

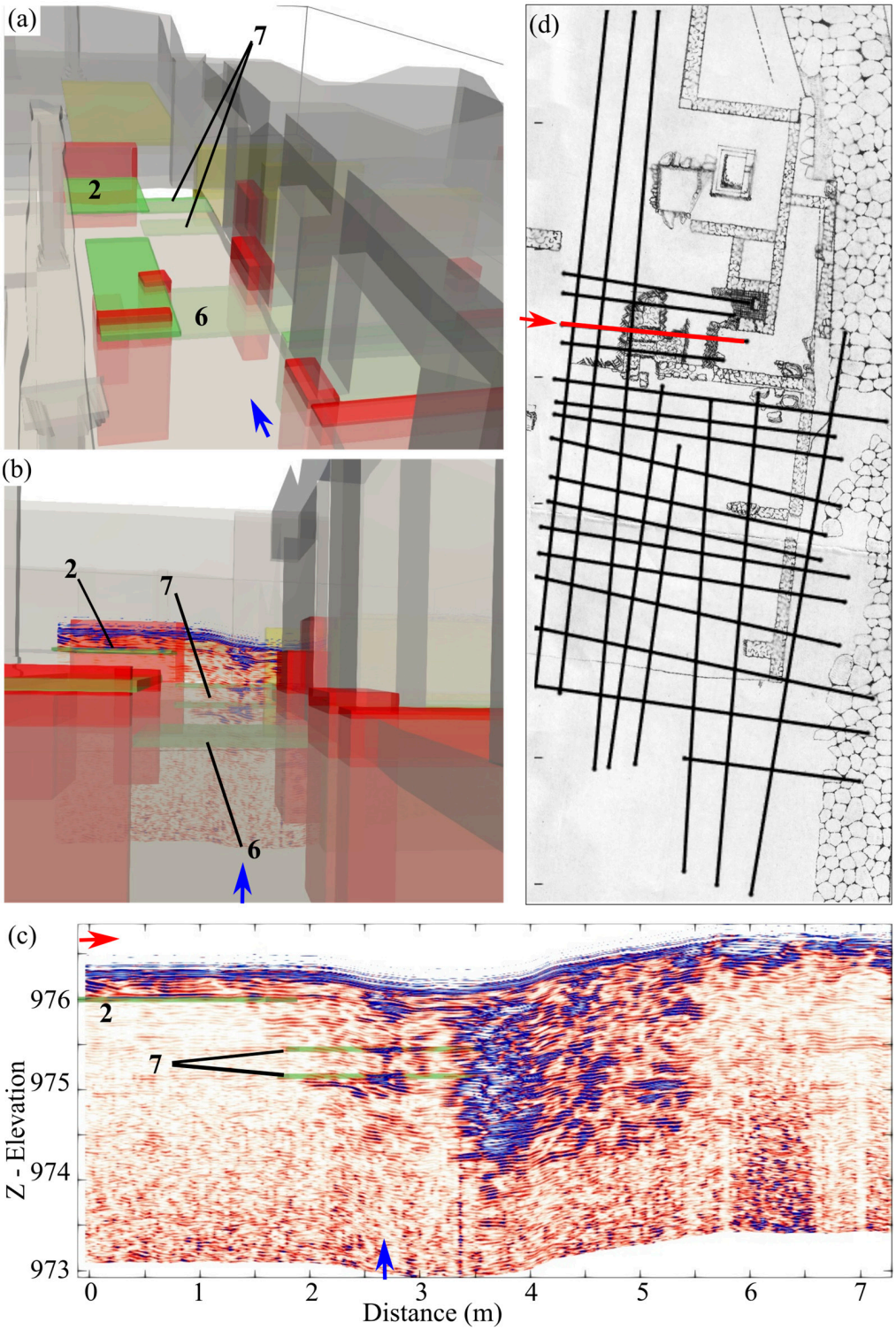


Figure 14. Close-up view of volume n. 7 (see also Figures 12 and 13 for the broader context). (**a**) View of a portion of the basilica 3D model is shown along with VOIs to highlight the agreement between the 3D building reconstruction and geophysical information. (**b**) Some of the volumes of interest together with the 3D model and the GPR scan (line no. 3) in which anomaly 7 is observed particularly well. (**c**) The B-scan acquired along line no. 3. (**d**) All the acquired lines. Line no. 3 is highlighted

in red. The GPR results were produced without any a priori knowledge. At a later stage, however, an excavation plan produced in 1988 became available. This plan is shown in the background to demonstrate that a buried stair is indeed present. Direction of the acquisition is indicated in (**c**,**d**) by the red arrows, while the blue arrows indicate the same viewing direction across the figures.

Furthermore, since not all anomalies are equally evident, a color-coding scheme was adopted to classify their significance: red to indicate anomalies for which the presence of a scattering body is considered certain, as indicated by strong and well-organized clusters of reflections; yellow to indicate anomalies characterized by weaker and less organized reflection patterns, requiring interpretative assessment (in other words "probable" anomalies); and green to mark anomalies associated with sparse, weakly organized reflection events, whose significance can be recognized only through expert analysis (i.e., "tentative" anomalies).

Figure 12a shows the integration of the architectural model and VOIs in the 3D environment. The location of the GOR survey is indicated with an arrow. Figure 12b,c provide combined views of the identified volumes and the VAM of the basilica, seen from the top and the side, respectively. Volumes of interest are numerically labeled, and the same labels are also used in Figures 13 and 14.

The following descriptions (corresponding to the labels in Figures 12–14) derive from our unbiased interpretation of the GPR data and were recorded without any previous knowledge of the site or the architectural model:

1. surface connecting several radar reflections, probably anomalies belonging to the ancient walking surface.
2. External walking surface, at a slightly lower level with respect to 1.
3. A set of internal walls. Radar anomalies in the B-scans presented as extremely strong and well-organized clusters of reflections, fading on both sides with relatively oblique diffraction hyperbolas. While difficult to interpret in the beginning, we soon realized that the fading hyperbolas were compatible with a configuration in which the path of the GPR antenna was slightly oblique with respect to the direction of the wall. Multiple scattering is a reasonable effect for walls built using irregularly shaped rocks of variable size. The findings reported in [32,33] have been particularly helpful in reaching this interpretation.
4. Anomalies belonging to an elongated structure, of which only two certain elements remain. Later on, this was associated with remains of the basilica external wall.
5. Possible buried remains of a wall. Some wall sections, perfectly in line with these anomalies, are still present.
6. Reflections indicating a surface corresponding to a deeper, possibly older, walking surface.
7. Volume containing a very complex reflection pattern that we hypothesized to belong to a stair.

To make sure that the geophysical interpretation was objective, all comparisons with other sources of information were performed a posteriori. Figure 13a shows an aerial view of the VOI overlaid with the orthophoto. It is noteworthy that the identified volumes are in remarkable agreement with the position of the visible remains, and several volumes look like natural continuations of the walls' remains. In a similar way, Figure 13b overlays the walls of the basilica 3D model on both VOI and orthophoto. The basilica model was developed in consultation with expert archeologists regarding ancient architectural styles and practices. A major role in its reconstruction was played by the assumption of symmetry with the western side of the building, which had been excavated years earlier and whose structure is well known. Alignment of the walls from the VAM with geophysical evidence is remarkable. Likewise, the vertical positions of the ancient pavements (labels 1 and 2)

were found to lie within 20 cm of the positions hypothesized by the VAM. Figure 13c,d offer additional views of VOIs. It could be observed in Figure 13d that the red anomalies seem to align, delineating a corridor-like space where reflections were almost absent, at the end of which a very complex reflection pattern is found.

Finally, Figure 14 highlights precisely this aspect. In Figure 14a, a detail of the 3D basilica model is compared with the volumes of interest. We now focus on the volume (or surfaces) labeled 7.

Figure 14b–d show the radar scans acquired progressively closer to the observer, starting from the anomaly location, in which this feature was identified. Due to the complexity of the multiple reflections and the presence of three signatures at slightly different depths, each becoming weaker as the antenna moved along lines progressively farther from them, we hypothesized the presence of a stairway, likely providing access to the deeper walking surface (6) and bounded by walls on each side.

It is worth emphasizing that this interpretation was tentative and made at a stage in which no external information was yet provided to the geophysical group. As such, volume no. 7 was highlighted in green. Nevertheless, prompted by our observations, our archeologists shared the plan in Figure 6. The map indeed shows that a stair was uncovered during an excavation in 1988 and subsequently re-covered to preserve the artifacts. The remarkable agreement of our tentative anomaly with an architectural detail so difficult to detect and the close agreement of the position of one of our probable (i.e., yellow) anomalies with a portion of wall that was actually found within the same excavation allows us to feel very confident about the interpretation of the anomalies marked in red, which are comparatively evident. In this paper, our anomaly search was primarily guided by expert interpretation. It is worth noting that alternative approaches do exist, such as time-reversal [34], full waveform inversion [35], and active surfaces [36,37]. The latter, in particular, will be the subject of future work

One may argue that the virtual architectural model does not fit the geophysical observation perfectly. Indeed, it must be emphasized that the VAM has been developed largely by leveraging visible evidence and partial archeological information, and has employed massively the idea of symmetry, as this concept was central to the Romans. In fairness, the full VAM offers an unprecedented view of the entire Iuvanum site, both for spatial extent and level of detail, and has played a central role in making sense of the GPR observations.

The basilica (i.e., a small portion of the VAM) has undergone several changes throughout history, so the introduction of asymmetrical elements is to be expected (e.g., Figure 13a,b). The GPR, on the other hand, allows us to detect such elements, regardless of the epoch of their construction.

5. Discussion and Conclusions

In this paper, we discuss two main aspects: one geophysical and one methodological. We combined the result of geomatic and geophysical observations to gain insight on the archeological site of Iuvanum (Chieti, Italy). To do so, we employed the ground-penetrating radar to probe the underground of a portion of the site where the ancient basilica once stood (one of the main buildings).

Unlike classic applications in the archeological context, our scans did not follow a regular grid (i.e., lines were neither parallel nor equally spaced and varied in length, leaving some gaps compared to a regular grid). As such, we could not rely on proper interpolation, and in turn, on the production of reliable C-scans. As an alternative, we created a three-dimensional representation of the radar scan. Additionally, topography had to be taken into account to better image buried reflectors. Consequently, the columns

of each GPR scan were shifted to account for elevation. Finally, the corrected B-scans were converted into 3D surfaces and assembled in a comprehensive three-dimensional view. This representation allowed us to cross-compare adjacent and intersecting B-scans, visualize in a unified framework reflection patterns and diffraction hyperbolas occurring along different directions, and ultimately identify volumes of interest delineating the likely location of the reflecting bodies, with different levels of certainty.

The contribution of geophysics was subsequently integrated, within the same three-dimensional framework, with the products from geomatics. In particular, the GPR was merged with the virtual architectural model (comprising models of buildings), DEM, and the orthophoto of the site.

From a geophysical perspective, we were able to clearly interpret all the observed anomalies and generate information that will become key in guiding future excavations, which ultimately are the only certain way to confirm the presence of buried remains. Initially, the interpretation was performed entirely on the basis of GPR data and without any other a priori information, in order to avoid bias. Our initial hypotheses were later confirmed by both prior excavation records of a small portion within the GPR survey (a report from 1988 that was disclosed afterwords) and by the axial symmetry of our VOI and elements on the opposite, excavated side of the basilica and the forum.

From a methodological perspective, we have created a comprehensive 3D framework where information from different sources can now coexist and be browsed simultaneously. Not only has this 3D framework proved to be remarkably versatile for interpreting the GPR B-scans, but the whole workflow is also flexible enough to allow the inclusion of C-scans (when available), as well as products from several other applied geophysical methods, provided that such products can be formatted in 3D.

Additionally, our approach of integrating different data within a comprehensive 3D environment is fully reproducible for other archeological sites, leaving ample scope for future applications in similar archeological contexts.

Author Contributions: All authors contributed to the conception and design of the study, the analysis and interpretation of the data, and the writing of the manuscript. M.P. and D.P. were responsible for the geomatic aspects, while S.B. led the geophysical components. Archeological expertise was provided by O.M. and P.S. All authors critically revised the manuscript for important intellectual content, approved the final version for publication, and agreed to be accountable for all aspects of the work. All authors have read and agreed to the published version of the manuscript.

Funding: This research was supported by the *Living forever the past through a 3Digital world*—Lip3D project (grant number 101173974) in the DIGITAL-2023-CLOUD-828 DATA-AI-05 program.

Data Availability Statement: The data supporting the findings of this study are available from the corresponding author upon request.

Acknowledgments: The authors gratefully acknowledge the anonymous reviewers for their valuable comments and constructive feedback which contributed to improving the manuscript.

Conflicts of Interest: The authors declare no conflicts of interest.

References

1. Zhao, W.; Forte, E.; Pipan, M.; Tian, G. Ground penetrating radar (GPR) attribute analysis for archaeological prospection. *J. Appl. Geophys.* **2013**, *97*, 107–117. [CrossRef]
2. Conyers, L.B. *Interpreting Ground-Penetrating Radar for Archaeology*; Routledge: London, UK, 2016.
3. Leckebusch, J. Ground-penetrating radar: A modern three-dimensional prospection method. *Archaeol. Prospect.* **2003**, *10*, 213–240. [CrossRef]
4. Gaffney, C.; Gater, J. *Revealing the Buried Past: Geophysics for Archaeologists*; Tempus: Stroud, UK, 2003.

5. Conyers, L.B.; Leckebusch, J. Geophysical archaeology research agendas: Ground-penetrating radar examples. *Archaeol. Prospect.* **2010**, *17*, 117–123. [CrossRef]
6. Daniels, D.J. *Ground Penetrating Radar*, 2nd ed.; IET: London, UK, 2004.
7. Neubauer, W. GIS in archaeology—The interface between prospection and excavation. *Archaeol. Prospect.* **2004**, *11*, 159–166. [CrossRef]
8. Patidar, A.K. An overview of the application of GPR Technology in Geotechnical and Geological Research: Examples from Gujarat, Western India. *Indian Geotech. J.* **2025**, *55*, 1255–1278. [CrossRef]
9. Tang, P.; Chen, F.; Jiang, A.; Zhou, W.; Wang, H.; Leucci, G.; de Giorgi, L.; Sileo, M.; Luo, R.; Lasaponara, R.; et al. Multi-frequency electromagnetic induction survey for archaeological prospection: Approach and results in Han Hangu Pass and Xishan Yang in China. *Surv. Geophys.* **2018**, *39*, 1285–1302. [CrossRef]
10. Persico, R.; Leucci, G.; Campana, S. Large-scale ground-penetrating radar surveys for the detection of buried archaeological structures. *Archaeol. Prospect.* **2022**, *29*, 493–507. [CrossRef]
11. Leucci, G. *Nondestructive Testing for Archaeology and Cultural Heritage*; Springer: Cham, Switzerland, 2019.
12. Masini, N.; Leucci, G.; Vera, D.; Sileo, M.; Pecci, A.; Garcia, S.; López, R.; Holguín, H.; Lasaponara, R. Towards urban archaeo-geophysics in Peru. The case study of plaza de armas in cusco. *Sensors* **2020**, *20*, 2869. [CrossRef]
13. Zaragoza, M.; Moyano, J.; Nieto-Julián, J.E.; León, J. Integration of geomatic and geophysical data for archaeological building modelling. *Sensors* **2024**, *24*, 642.
14. Fiedler, S.; Illich, B.; Berger, J.; Graw, M. The effectiveness of ground-penetrating radar surveys in locating unmarked graves. *J. Appl. Geophys.* **2009**, *68*, 380–385. [CrossRef]
15. Al-Assadi, H.A.; Abd, N.A. Application of georadar method to investigate shallow artifacts for Al-Maabid area in Babylon archaeological city. *Iraqi Geol. J.* **2023**, *57*, 288–295. [CrossRef]
16. Kareem, H.A.; Abd, N.A. Detection of subsurface archaeological features using the GPR method with a 250 MHz antenna in Borsippa site, Babylon, Iraq. *Iraqi J. Sci.* **2024**, *65*, 9694. [CrossRef]
17. Piroddi, L.; Rassu, M. Application of GPR prospection to unveil historical stratification inside monumental buildings: San Leonardo de Siete Fuentes, Italy. *Land* **2023**, *12*, 590. [CrossRef]
18. Paoletti, V.; La Manna, M.; Capozzoli, A.; Mercurio, M.; Zinni, M.; Naso, A. GPR Survey at the Etruscan Necropolis of Sasso Pinzuto, Tuscania (Central Italy). *J. Archaeol. Sci. Rep.* **2024**, *60*, 104833. [CrossRef]
19. Kirchhöfer, M.; Chandler, J.; Wackrow, R. Cultural Heritage Recording Utilising Low-Cost Close-Range Photogrammetry. *Geoinformatics FCE CTU* **2011**, *6*, 185–192. [CrossRef]
20. Fabbricotti, E. Storia di un tratturo. In *Settlement and Economy in Italy 1500 BC to AD 1500*; Archaeopress: Oxford, UK, 1995; pp. 197–199.
21. Menozzi, O.; Fossataro, D. Iuvanum Survey Project: I dati del territorio. In *Iuvanum. L'area Archeologica*; Synapsi: Edizioni, Italy, 2006; pp. 31–37.
22. Menozzi, O. New technologies and traditional approaches in reconstructing the ancient landscape assessment. In *Proceedings of the IX Symposium of Mediterranean Archaeology*; British Archaeological Reports: Oxford, UK, 2008; pp. 39–62.
23. Fabbricotti, E. Il sito di Iuvanum. In *Atti del Convegno Iuvanum 1990, Chieti, Italy*; Solfanelli: Chieti, Italy, 1983; pp. 9–18.
24. Fabbricotti, E. Cambiamenti di vita ad Iuvanum. In *New Developments in Italian Archaeology*; Oxbow Books: Oxford, UK, 1992; pp. 77–82.
25. Bradley, G.; Fossataro, D.; Menozzi, O.; Antonelli, S.; Mancini, M.C. Iuvanum Survey Project: Report and Results. *Quad. Archeol. D'abruzzo Not. Della Soprintend. Beni Archeol. Dell'abruzzo* **2011**, *3*, 19–38.
26. Klapa, P.; Żygadło, A.; Pepe, M. 3D heritage reconstruction through HBIM and multi-source data fusion: Geometric change analysis across decades. *Appl. Sci.* **2025**, *15*, 8929. [CrossRef]
27. Martino, A.; Gerla, F.; Balletti, C. Multi-Scale and Multi-Sensor Approaches for the Protection of Cultural Natural Heritage: The Island of Santo Spirito in Venice. *Int. Arch. Photogramm. Remote Sens. Spat. Inf. Sci.* **2023**, *48*, 1027–1034. [CrossRef]
28. Bitelli, G.; Barbieri, E.; Girelli, V.A.; Lambertini, A.; Mandanici, E.; Melandri, E.; Ugolini, A. The Complex of Santa Croce in Ravenna as a Case Study: Integration of 3D Techniques for Surveying and Monitoring of a Historical Site. In *Proceedings of the ARQUEOLÓGICA 2.0—9th International Congress & 3rd GEORES—GEOmatics and pREServation*; Editorial of the Universitat Politècnica de València: València, Spain, 2021; pp. 408–413.
29. Sandmeier, K.J. *ReflexW Version 8.1: Program for Processing of Seismic, Acoustic or Electromagnetic Reflection, Refraction and Transmission Data*; Software Manual: Karlsruhe, Germany, 2016; 628p.
30. Schroeder, W.; Martin, K.; Lorensen, B. *The Visualization Toolkit*, 4th ed.; Kitware: Clifton Park, NY, USA, 2006; ISBN 978-1-930934-19-1.
31. Ahrens, J.; Geveci, B.; Law, C. ParaView: An End-User Tool for Large Data Visualization. In *The Visualization Handbook*; Elsevier: Amsterdam, The Netherlands, 2005; pp. 717–731, ISBN 978-0123875822.
32. Thakur, M.M.; Prashant, A. GPR Signatures of Pipes and Walls with Emphasis on the Effect of Inclined Scanning Trajectory. *Geotech. Geol. Eng.* **2017**, *35*, 1977–1989. [CrossRef]

33. Negri, S.; Aiello, M.A. High-resolution GPR survey for masonry wall diagnostics. *J. Build. Eng.* **2021**, *33*, 101817. [CrossRef]
34. Sajjad, G.; Hafizi, M.K.; Bano, M.; Ebrahimi, A. Application of Time Reversal (TR) Imaging to GPR Data for Detecting an Avalanche Victim. *Arab. J. Geosci.* **2022**, *15*, 517. [CrossRef]
35. Lavoué, F.; Brossier, R.; Métivier, L.; Garambois, S.; Virieux, J. Two-dimensional permittivity and conductivity imaging by full waveform inversion of multioffset GPR data: A frequency-domain quasi-Newton approach. *Geophys. J. Int.* **2014**, *197*, 248–268. [CrossRef]
36. Bignardi, S.; Yezzi, A.J.; Yildirim, A.; Barnes, C.F.; Sandhu, R. A feasibility study of radar-based shape and reflectivity reconstruction using variational methods. *Inverse Probl.* **2021**, *37*, 025004. [CrossRef]
37. Bignardi, S.; Sandhu, R.; Yezzi, A. Radar-Based Shape and Reflectivity Reconstruction Using Active Surfaces and the Level Set Method. *IEEE Trans. Pattern Anal. Mach. Intell. (TPAMI)* **2023**, *45*, 3617–3631. [CrossRef]

Disclaimer/Publisher's Note: The statements, opinions and data contained in all publications are solely those of the individual author(s) and contributor(s) and not of MDPI and/or the editor(s). MDPI and/or the editor(s) disclaim responsibility for any injury to people or property resulting from any ideas, methods, instructions or products referred to in the content.